Virology 476 (2015) 168–179

Contents lists available at ScienceDirect

Virology

journal homepage: www.elsevier.com/locate/yviro

Daclatasvir inhibits hepatitis C virus NS5A motility and hyper-accumulation of phosphoinositides

Vineela Chukkapalli [a], Kristi L. Berger [a,1], Sean M. Kelly [a], Meryl Thomas [b], Alexander Deiters [b], Glenn Randall [a,*]

[a] Department of Microbiology, The University of Chicago, Chicago, IL 60637, USA
[b] Department of Chemistry, University of Pittsburgh, Pittsburgh, PA 15260, USA

ARTICLE INFO

Article history:
Received 4 December 2014
Accepted 9 December 2014
Available online 26 December 2014

Keywords:
Phosphatidylinositol-4-kinase alpha
Phosphatidylinositol-4-phosphate
HCV replication complex
Direct-acting anti-virals

ABSTRACT

Combinations of direct-acting antivirals (DAAs) against the hepatitis C virus (HCV) have the potential to revolutionize the HCV therapeutic regime. An integral component of DAA combination therapies is HCV NS5A inhibitors. It has previously been proposed that NS5A DAAs inhibit two functions of NS5A: RNA replication and virion assembly. In this study, we characterize the impact of a prototype NS5A DAA, daclatasvir (DCV), on HCV replication compartment formation. DCV impaired HCV replicase localization and NS5A motility. In order to characterize the mechanism behind altered HCV replicase localization, we examined the impact of DCV on the interaction of NS5A with its essential cellular cofactor, phosphatidylinositol-4-kinase III α (PI4KA). We observed that DCV does not inhibit PI4KA directly, nor does it impair early events of the NS5A–PI4KA interaction that can occur when NS5A is expressed alone. NS5A functions that are unaffected by DCV include PI4KA binding, as determined by co-immunoprecipitation, and a basal accumulation of the PI4KA product, PI4P. However, DCV impairs late steps in PI4KA activation that requires NS5A expressed in the context of the HCV polyprotein. These NS5A functions include hyper-stimulation of PI4P levels and appropriate replication compartment formation. The data are most consistent with a model wherein DCV inhibits conformational changes in the NS5A protein or protein complex formations that occur in the context of HCV polyprotein expression and stimulate PI4P hyper-accumulation and replication compartment formation.

Introduction

About 150 million people are chronically infected with hepatitis C virus (HCV) (WHO). Therapy for HCV including interferon and ribavarin and a viral protease inhibitor boceprevir or telapravir, is successful in ~75% of treatments (Chatel-Chaix et al., 2012). Recently, simeprevir, another protease inhibitor and sofosbuvir, a nucleotide analog inhibitor of the viral polymerase were also approved for therapy and improvement of response rates (Stedman, 2014). Many interferon-free regimens combining different DAA classes are currently in clinical trials (Au and Pockros, 2014). A common component of these combination therapies is the NS5A DAA, typified by the lead compound daclatasvir (DCV). DCV has currently moved to Phase III trials and is noteworthy due to its very high potency (picomolar) against HCV in vitro as compared with other HCV inhibitors (Gao et al., 2010). The mechanism of action for this drug class is unclear; however, it is thought to target HCV NS5A since drug resistant mutations accumulate in the viral NS5A gene (Lemm et al., 2010). NS5A DAAs block HCV at two different stages of life cycle with distinct kinetics: HCV replication complex formation and assembly of infectious HCV particles (McGivern et al., 2014; Guedj et al., 2013).

NS5A is a multi-functional protein with roles in HCV replication and virion assembly (Appel et al., 2008; Penin et al., 2004; Lohmann et al., 2003; Blight et al., 2000). It binds RNA and interacts with several cellular factors to establish an environment conducive for virus replication (Moradpour and Penin, 2013; He et al., 2006). Two phosphorylated forms of NS5A, a basally phosphorylated p56 form and a hyper-phosphorylated form p58, exist in infected cells (Kaneko et al., 1994). It has been suggested that the ratio between these two forms is crucial for both replication and assembly of the virus (Evans et al., 2004; Huang et al., 2007). HCV replicon cells treated with DCV have reduced hyper-phosphorylated NS5A (Lemm et al., 2010; Qiu et al., 2011). It is unclear whether this loss of hyper-phosphorylated NS5A is due to the direct inhibition of a kinase that phosphorylates NS5A or is due to an indirect effect mediated by the inhibition of HCV replication. In addition to the lack of hyper-phosphorylated NS5A, DCV-treated cells also show altered sub-cellular localization of NS5A

* Correspondence to: Department of Microbiology The University of Chicago, CLSC 707B, 920 East 58th Street, Chicago, Illinois 60637, USA. Tel.: +1 773 702 5673; fax: +1 773 834 8150.
E-mail address: grandall@bsd.uchicago.edu (G. Randall).
[1] Present address: Boehringer Ingelheim Pharmaceuticals, Inc., 900 Ridgebury Road, Ridgefield, CT 06877, USA.

http://dx.doi.org/10.1016/j.virol.2014.12.018
0042-6822/

but the mechanism of this mislocalization is unknown (Lee et al., 2011; Targett-Adams et al., 2011).

One major function of NS5A is to recruit and activate the cellular kinase phosphatidylinositol-4-kinase alpha (PI4KA) (Reiss et al., 2011; Berger et al., 2011; Tai and Salloum, 2011 ; Bianco et al., 2012; Reiss et al., 2013). PI4KA and potentially its product phosphatidylinositol-4-phosphate (PI4P) are critical for HCV replication (Berger et al., 2009; Tai et al., 2009; Li et al., 2009; Borawski et al., 2009; Trotard et al., 2009; Vaillancourt et al., 2009; Berger and Randall, 2009). In the absence of PI4KA, non-structural proteins form enlarged cytoplasmic structures suggesting improper formation of replication compartments (Reiss et al., 2011; Berger et al., 2011; Tai and Salloum, 2011; Wang et al., 2014). Interestingly, we observed a similar phenotype in DCV-treated cells, leading to the hypothesis that DCV may be altering NS5A–PI4KA interaction and/or activation. To test this hypothesis, we relied on a Tet-inducible osteosarcoma cell line (UHCV) that expresses full-length viral proteins independent of replication (Moradpour et al., 1998). We have previously reported that sole expression of NS5A in this system weakly induces PI4P accumulation, while PI4P is highly induced in the context of the HCV polyprotein (Berger et al., 2011). This observation is consistent with the recent data that NS5B in addition to NS5A is required to observe maximally elevated levels of PI4P in cells (Reiss et al., 2013). In this study, we present evidence that DCV blocks replicase formation and the hyper-induction of PI4P by the HCV polyprotein, but not basal activation of PI4KA by NS5A alone. These data lead to a model wherein NS5A alone can bind and weakly activate the kinase in the presence of DCV, but that DCV inhibits an NS5A conformational change that occurs in the context of the HCV polyprotein and is associated with both PI4P hyper-accumulation and HCV replication complex formation.

Results

Daclatasvir treatment results in large replicase protein structures with morphology similar to those in cells treated with PI4KA siRNAs

DCV has been shown to cause NS5A relocalization (Lee et al., 2011; Targett-Adams et al., 2011). To determine if other non-structural proteins also relocalize in the presence of DCV, we used cells that express HCV polyprotein independent of replication to monitor replication compartment formation. U2OS osteosarcoma cells expressing full-length HCV polyprotein under tetracycline-inducible conditions (UHCV cells) have been previously used to identify and describe the formation of HCV replication compartments, the membranous web (Moradpour et al., 1998; Gosert et al., 2003). UHCV cells were induced for HCV polyprotein expression in the presence of DMSO or DCV (250 pM), then probed for NS5A and NS5B (the polymerase) localization in UHCV (Fig. 1) In DMSO-treated cells, NS5B shows evenly distributed reticular pattern as observed previously (Berger et al., 2011). However, in DCV-treated cells, NS5B forms large aggregated structures that co-localize with NS5A. PI4KA siRNA-treatment of cells leads to similar aggregation of replicase proteins and alters membranous web morphology (Reiss et al., 2011; Berger et al., 2011; Tai and Salloum, 2011). The similar phenotypes observed between PI4KA siRNA-treated cells and DCV-treated cells lead to a hypothesis of parallel mechanism of action, whereby DCV may perturb HCV-stimulated PI4P accumulation.

Daclatasvir reduces NS5A motility and increases NS5A puncta intensity

To better understand the nature of the large NS5A puncta, we examined the effects of DCV on NS5A dynamics in HCV-infected

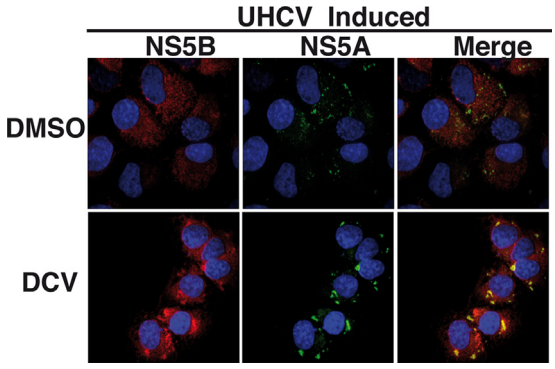

Fig. 1. DCV causes aggregation of replicase proteins. UHCV cells were induced and treated with DMSO or DCV (250 pM) for 72 h and probed for NS5B (red) and NS5A (green). Note the aggregated staining of both NS5A and NS5B in DCV-treated cells.

cells. NS5A has been reported to have two dynamic patterns consisting of smaller motile structures and larger, less motile structures (Eyre et al., 2014; Wolk et al., 2008). We constructed an HCV JC1-like virus (NS2/3) with an eYFP insertion in the C-terminal domain of NS5A, termed NS2/3 5A-eYFP similar to what has been previously described (Moradpour et al., 2004). For efficient replication, residues 2242–2266 in NS5A domain II were deleted (NS2/3 5AΔ25-eYFP) (Fig. 2A) (Gottwein et al., 2011). This virus replicated similar to wild type HCV and was sensitive to DCV treatment (Fig. 2B). We next performed live-cell imaging of NS2/3 5 AΔ25-eYFP infected cells that were treated with DCV or DMSO and imaged after 3, 8 or 24 h (Movies S1–S4). The total distance traveled (including progressive and non-progressive movement) by NS5A puncta over 15 min periods was quantified. Three representative particle tracks for DMSO and 24 h post DCV treatment are shown in Fig. 2C. As quantified in Fig. 2D, by 8 h post DCV treatment, the total distance traveled by NS5A puncta is reduced and by 24 h, it is significantly lower as compared to the DMSO control. There was a significant increase in the NS5A fluorescence intensities by 24 h post DCV treatment, consistent with the kinetics of replicase aggregation observed in Fig. 1 (Fig. 2E). It should be noted however that the increase in NS5A fluorescent intensities is not due to increase in protein levels but rather due to aggregation of NS5A fluorescent signal. Indeed, as expected, steady-state NS5A levels are decreased upon DCV treatment due to the inhibition of replication (Fig. 2F).

Daclatasvir inhibits HCV-induced PI4P accumulation

The aggregation of non-structural proteins in the presence of DCV is similar to that observed in cells treated with siRNAs against PI4KA, suggesting that DCV might be altering the NS5A–PI4KA interaction. To determine whether DCV inhibits NS5A-mediated PI4P accumulation, we induced UHCV cells for polyprotein expression and treated them simultaneously with either DMSO or DCV for 72 h. As seen in Fig. 3A, uninduced UHCV cells show PI4P localization restricted to Golgi, as indicated by colocalization of PI4P with the Golgi marker GM130. Upon HCV polyprotein induction, greater that 80% of cells have PI4P accumulation away from Golgi (Fig. 3B), as previously described (Berger et al., 2011). However, when cells were treated with DCV during polyprotein synthesis, PI4P intensity is significantly reduced (Fig. 3C) and only about 15% of cells showed PI4P relocalization away from Golgi (Fig. 3B). This lack of HCV-mediated PI4P synthesis in DCV-treated cells is not due to the decreased polyprotein expression. Although DCV treatment altered NS5A localization, as in Figs. 1 and 3D, similar levels of NS5A are observed in both DMSO and DCV-treated

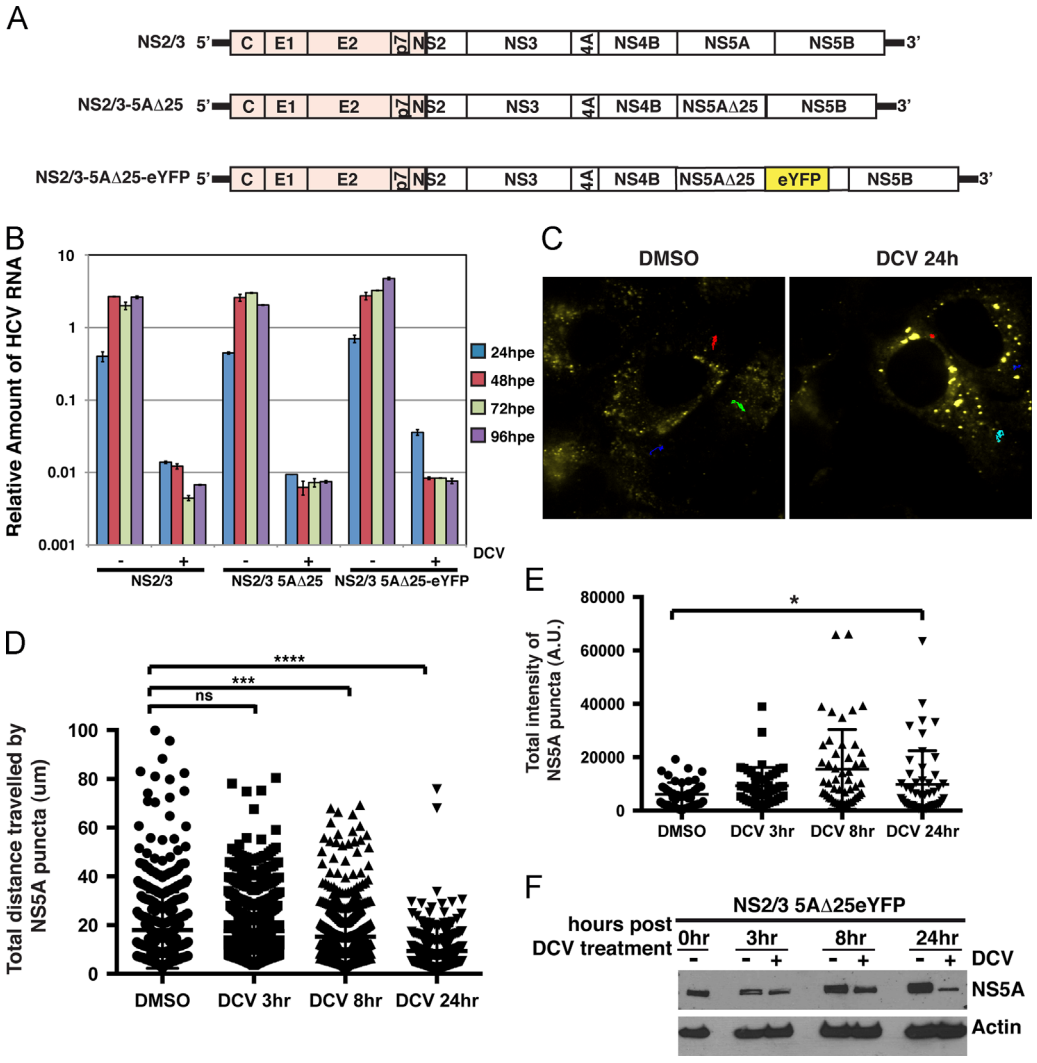

Fig. 2. DCV causes reduction in NS5A movement and an increase in NS5A intensity. (A) Schematic of WT, NS5A deletion and NS5A-eYFP NS2/3 constructs (shaded structural region is from J6 genotype while the non-structural regions are from JFH1 genotype). (B) Huh-7.5 cells were electroporated with in vitro transcribed RNA from the constructs described in panel A. and either DMSO or DCV (1 nM) was added to cells at 4 h post-electroporation (hpe). RNA was collected at 4, 24, 48, 72, and 96 hpe and analyzed by quantitative RT-PCR, normalizing to RNA levels at 4hpe. (C–E) Huh-7.5 cells were infected with NS2/3 NS5AΔ25-eYFP virus. 48 post-infection (hpi), cells were treated with DMSO or DCV (500 pM) and monitored at 3, 8 and 24 h post-treatment using confocal microscopy. Images were taken every 20 s for a total of 15 min. (C) Representative tracks of 3 particles for DMSO and DCV-treated cells are shown. (D) Total distance traveled by NS5A-YFP puncta was calculated using Image J multi-tracker plugin. Each dot represents the total distance traveled by individual puncta. (E) NS5A puncta intensity (integrated density) was calculated by using Manual multiple ROI analysis. ns, not significant; $^{*}p < 0.05$; $^{***}p < 0.001$; $^{****}p < 0.0001$. (F) Cells were treated as in C and cell-lysate was run on SDS-PAGE and blotted for NS5A and Actin.

cells as analyzed by Western blot (Fig. 3E). Altogether, these data suggest that DCV inhibits HCV-mediated PI4P hyper-induction and relocalization.

Daclatasvir does not alter plasma membrane PI4P levels and is thus unlikely to inhibit PI4KA directly

PI4KA is required to maintain plasma membrane pools of PI4P (Balla et al., 2005). To determine whether DCV inhibits PI4KA directly, we analyzed plasma membrane PI4P levels as described in materials and methods, using distinct permeabilization conditions from that used in Fig. 3 to visualize intracellular PI4P levels. UHCV cells were induced or left uninduced for 72 h and treated with DMSO (72 h), DCV (72 h) or the general PI kinase inhibitor wortmannin (30 min) prior to probing for plasma membrane pools of PI4P. As seen in Fig. 4A, there is significant staining of plasma membrane with the PI4P antibody in both induced and uninduced cells, which is different from the intracellular Golgi localization observed in Fig. 3. PI4P colocalizes to some extent with wheat-germ agglutinin, which binds to lectins and acts as a marker for the plasma membrane. There is however no significant difference between plasma membrane intensity of PI4P in DMSO and DCV-treated cells, whereas plasma membrane intensity of PI4P is significantly diminished in cells treated with wortmannin at a concentration (10 μM) that is known to inhibit PI4KA (Fig. 4A and B). Altogether, these data suggest that DCV does not block PI4KA activity directly but may block activation of PI4KA by NS5 A.

Daclatasvir does not inhibit PI4P relocalization mediated by NS5A alone

Given that DCV prevented PI4P hyper-accumulation in cells expressing full-length HCV polyprotein, we next examined whether DCV impacts the modestly enhanced stimulation of PI4P accumulation observed in cells expressing NS5A alone (Reiss et al., 2011; Berger et al., 2011). Induction of NS5A in UNS5A cells moderately stimulates PI4P accumulation (~1.5-fold, Fig. 5A

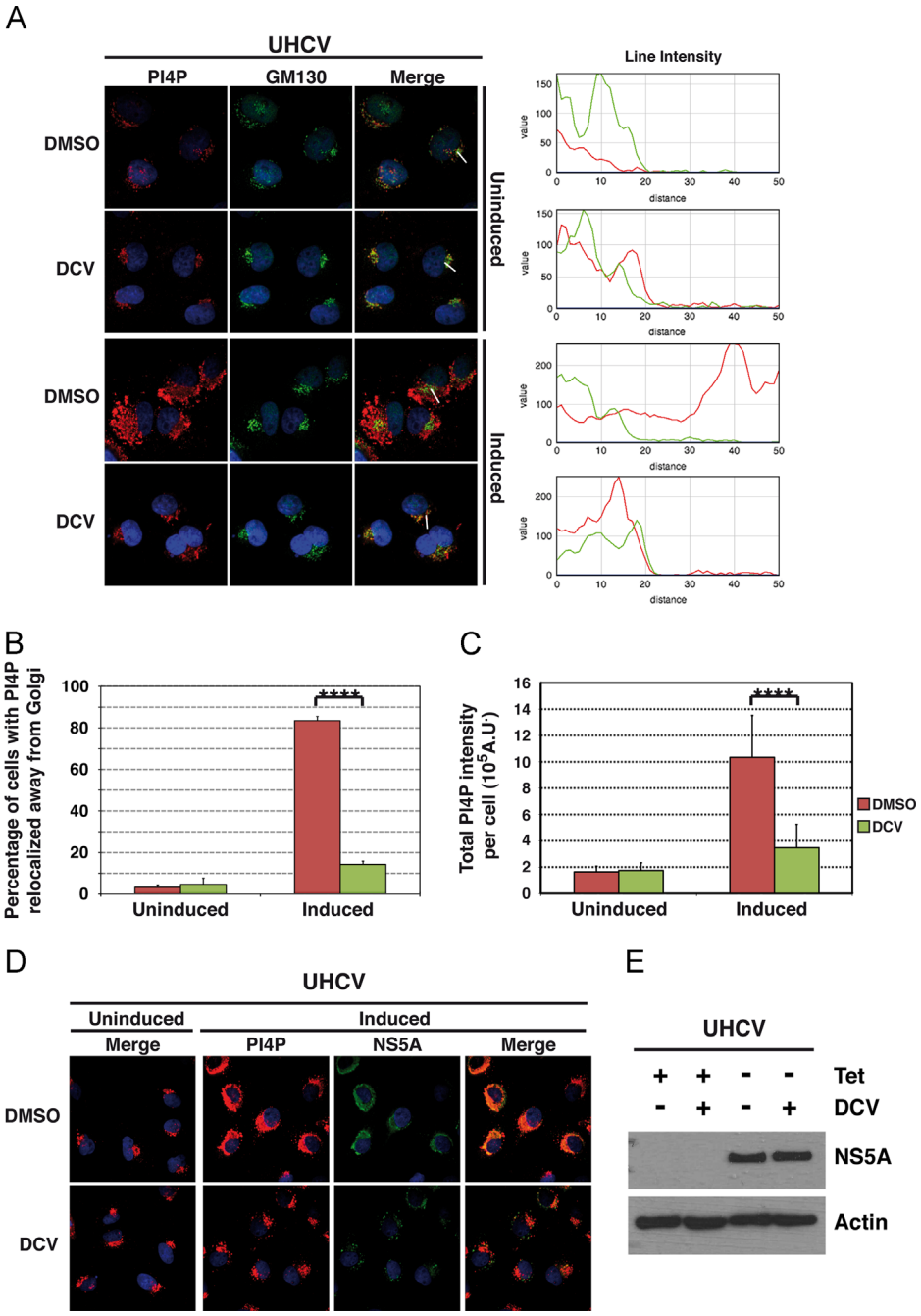

Fig. 3. DCV prevents HCV polyprotein-mediated PI4P production. (A) UHCV cells were induced for HCV polyprotein synthesis or uninduced for 72 h and then were treated with DMSO or DCV (250 pM) during the induction time. Cells were then fixed and probed for PI4P (red) and GM130 (green). Image J color intensity plots for the white line drawn in the merge image are shown on the right. (B) Quantification of cells showing relocalization in each condition from three independent experiments is shown on the bottom panel ($n=15$ fields ranging from 40 to 60 cells/condition/experiment). Cells with more than 5 PI4P puncta above threshold signal away from Golgi (based on GM130 signal) were quantified as positive for relocalization. Error bars represent standard deviation between three independent experiments. (C) PI4P intensity levels per cell were calculated using Image J. (D) Cells were treated as above and detected using indirect immunofluorescence via sequential staining first for NS5A (green) and then for PI4P (red). (E) Cells were treated as in A and cell-lysate was run on SDS-PAGE and blotted for NS5A and Actin. ****$p<0.0001$.

and C), albeit not as efficiently as observed in UHCV cells (~6-fold, Fig. 3A and C), even though, similar or more NS5 A is expressed in the conditions tested (Fig. 3E. versus Fig. 5E.). This data suggests that other HCV proteins may also have a role in modulating PI4P accumulation, either directly or indirectly. When NS5A is expressed alone, PI4P relocalization away from the Golgi (as seen in line intensity plots) is similar in DMSO- and DCV-treated cells suggesting that DCV is unable to block the initial PI4P relocalization mediated by NS5A (Fig. 5A). The number of cells showing PI4P relocalization is also not significantly different between DMSO and DCV-treated conditions (Fig. 5B). In contrast to UHCV cells, no difference in NS5A localization was observed in UNS5A cells in the presence of DCV (Fig. 5D). Steady state NS5A levels are also similar in DMSO- and DCV-treated cells (Fig. 5E).

Biotinylated NS5A inhibitor interacts with NS5A at similar efficiency in both UHCV and UNS5A cells

A biotinylated DCV-like drug has been used before for NS5A interaction studies and the structural comparison between DCV and

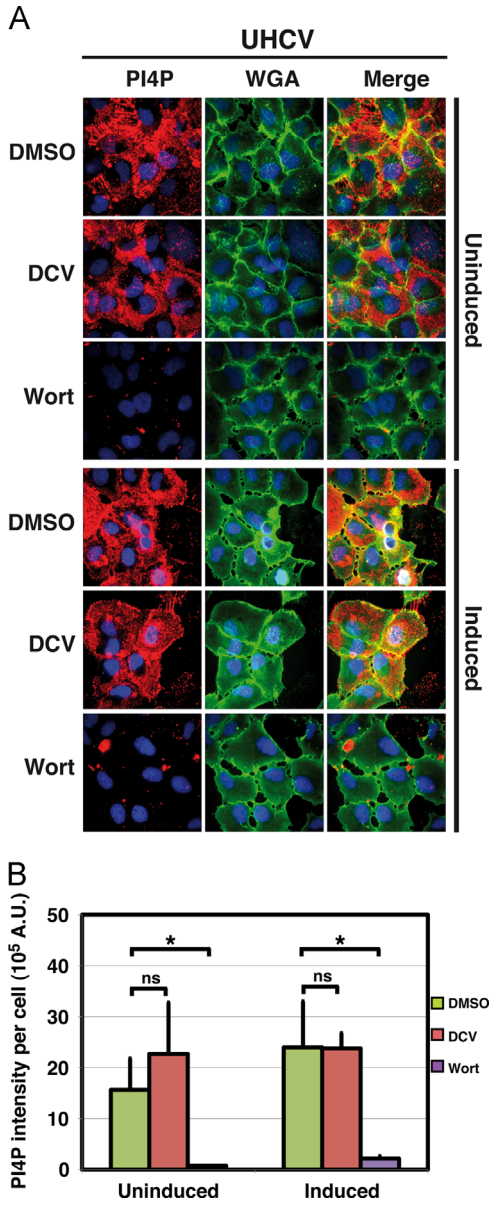

Fig. 4. DCV does not inhibit plasma membrane PI4P levels that are maintained by PI4KA. UHCV cells were induced or uninduced for a total of 72 h. Cells were either treated with DMSO or 250 pM DCV for 24 h or 10 μM wortmannin for 2 h, prior to incubating with 50 μg/ml Alexa Fluor 488-Wheat Germ Agglutinin on ice for 5 min to mark cell surface. Cells were then fixed and stained for plasma membrane PI4P. (A) Z-stack images across the plane of the cell were taken using confocal microscope and the maximum intensity projection image is shown. (B) Quantification of PI4P intensity per cell is shown. Error bars represent standard deviation between cells. ns, not significant; $^{*}p < 0.05$.

the tagged NS5A inhibitor is shown (Fig. 6A) (Gao et al., 2010). Though not as potent inhibitor as DCV, this tagged NS5A inhibitor still inhibits HCV replication (Fig. 6B). To determine whether the drug binds NS5A expressed from both UHCV and UNS5A cells, a biotin-tagged NS5A inhibitor was incubated with induced or uninduced cells for 16 h before lysis. The biotinylated drug was then pulled down with streptavidin beads overnight, washed and analyzed for NS5A that was pulled down using western blotting. As seen in Fig. 6C, the biotinylated drug precipitates NS5A at similar efficiency in both UHCV and UNS5A cells. Thus, the inability to block PI4P relocalization is not due to the inability of the drug to interact with NS5A in UNS5A cells. Based on these data, it is likely that DCV does not inhibit moderate PI4KA stimulation seen in cells expressing NS5A alone but inhibits hyper-accumulation of PI4P observed only in the context of HCV polyprotein expression.

Daclatasvir functions after NS5A–PI4KA interaction

In order to further analyze the mechanism by which DCV inhibits PI4P production in UHCV cells, we tested whether NS5A and PI4KA still interact in the presence of DCV. UHCV cells were transduced with lentiviral pseudoparticles expressing HA-tagged PI4KA and twenty-four hours later, cells were stimulated for HCV protein expression. Cells were then treated for 24 h with DMSO or DCV (250 pM) on day 3 and lysed and immunoprecipitated either using HA or NS5A antibody. NS5A co-immunoprecipitated with PI4KA and vice versa in DMSO-treated cells as previously described (Fig. 7). PI4KA still co-immunoprecipitates with NS5A in DCV-treated cells, suggesting that the interaction between NS5A and PI4KA remains intact even in the presence of DCV. Similar observations were made with endogenous PI4KA (data not shown). Thus, it is likely that DCV functions subsequent to the initial NS5A–PI4KA interaction (Fig. 6) and basal stimulation of PI4KA activity (Fig. 5), but prior to the hyper-stimulation of PI4KA (Figs. 1–3).

Daclatasvir resistant mutants rescue PI4P production

We next tested whether a DCV-resistant mutant could rescue PI4P accumulation in DCV-treated cells. Huh-7.5 cells were infected with either WT or DCV-resistant Y93H virus. Forty-eight hours post-infection, cells were treated with DMSO (data not shown) or 500 pM DCV and fixed at 2, 6, and 24 h post-treatment and probed for PI4P and NS5A (Fig. 8A and B). Cells infected with WT virus showed significant reduction in PI4P levels starting at 6 h post DCV treatment. At around the same time, NS5A begins to aggregate which is further increased by 24 h post-treatment. This NS5A aggregation seems to correlate to what was observed in DCV-treated UHCV cells (Fig. 1), live-cell analysis (Fig. 2) and in siPI4KA-treated cells (Berger et al., 2011). The DCV-resistant mutant Y93H-infected cells, on the other hand, had enhanced PI4P accumulation in the presence of DCV and no significant difference was observed between the time points (Fig. 8A and B). Similar to previous observations, this mutant also rescues NS5A localization (Targett-Adams et al., 2011). Thus, the drug-resistant mutant is able to rescue PI4P production in the presence of DCV. Consistent with NS5A aggregation and loss of PI4P levels that are indicative of replication inhibition, NS5A levels were also reduced by 24 h in WT but not in the resistant Y93H virus infected cells (Fig. 8C). Hyperphosphorylated NS5A decreased with greater kinetics than hypophosphorylated NS5A DCV treatment for WT virus (Fig. 8C). This suggests that either DCV directly inhibits NS5A phosphorylation, or alternatively, that hyperphosphorylated NS5A has a shorter half-life and hypophosphorylated NS5A and that its preferential decrease is an indirect effect of inhibiting HCV replication.

In order to verify the above data in replication-independent mechanism, we switched to transient transfection of NS3-5b in T7RP cells instead of using UHCV cells, since NS5A hyperphosphorylation is not readily distinguished in UHCV cells. T7RP cells were transfected with NS3-5B expression plasmid containing either WT, DCV-resistant mutant Y93H or PI4KA-interaction mutant HIT-AAA of NS5A. Four hours post-transfection, cells were treated with DMSO or DCV (500 pM or 5 nM) and either fixed or lysed at 24 h post-transfection. Similar to UHCV and virus infection data, DCV inhibited PI4P levels in WT NS5A expressing cells (Fig. 9A and B). The Y93H mutant, on the other hand, did not show any significant changes in PI4P levels even with high concentrations of PI4P. The PI4KA-interaction mutant, HIT-AAA, as expected did not show any increase

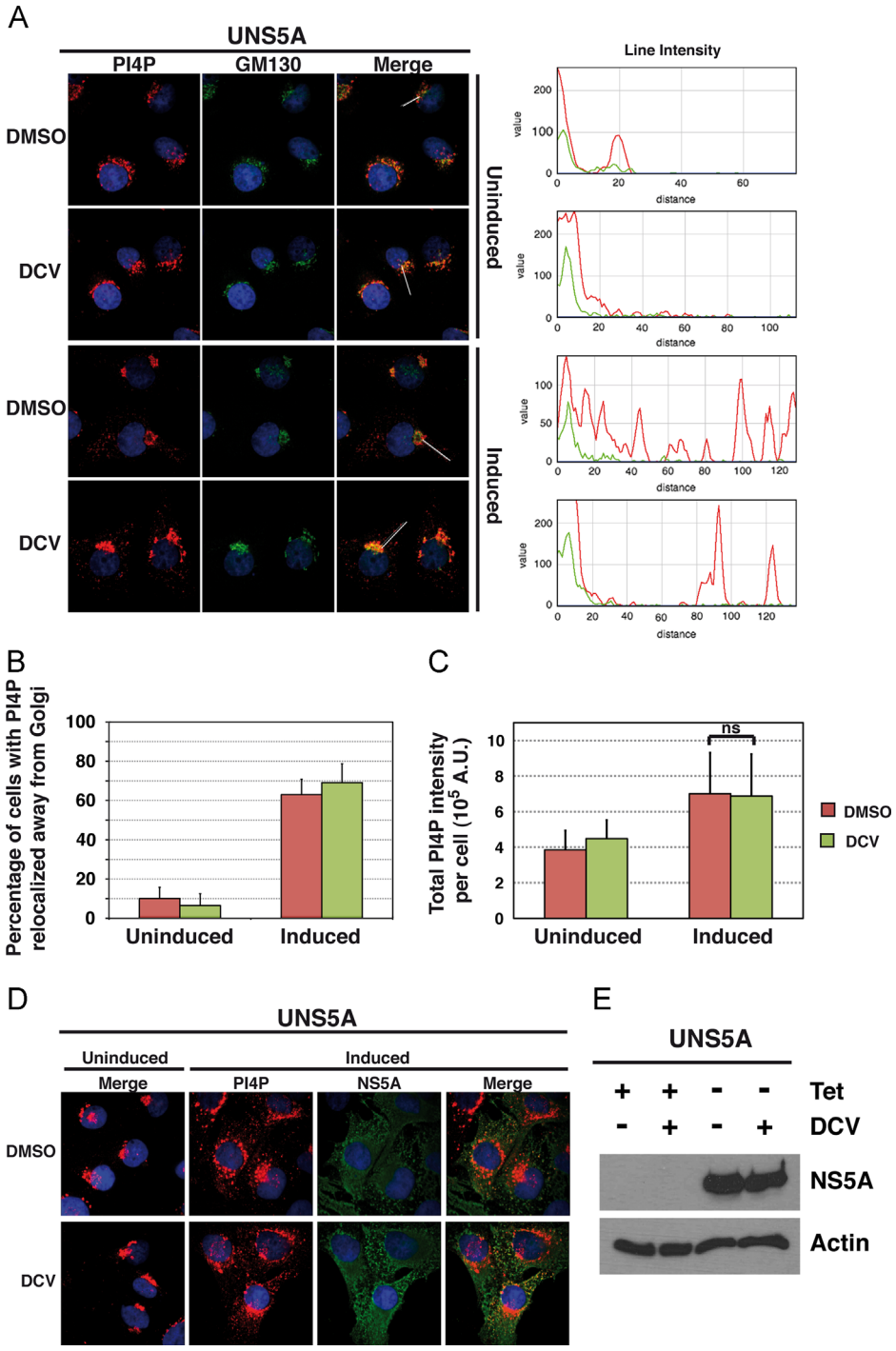

Fig. 5. DCV does not prevent NS5A-mediated PI4P relocalization. (A) UNS5A cells were induced for HCV NS5A synthesis or uninduced for 92 h in the presence of DMSO or DCV (250 pM). Cells were then fixed and probed for PI4P (red) and GM130 (green) and analyzed as in Fig. 3A. Image J color intensity plots for the white line drawn in the merge image are shown on the right. (B) Quantification of cells showing relocalization in each condition from three independent experiments is shown on the bottom panel ($n=15$ fields ranging from 40 to 80 cells/condition/experiment). Cells with more than 5 PI4P puncta above threshold signal away from Golgi (based on GM130 signal) were quantified as positive for relocalization. Error bars represent standard deviation between three independent experiments. (C) PI4P intensity levels per cell were calculated using Image J and plotted. (D) Cells were treated as above and detected using indirect immunofluorescence via sequential staining first for NS5A (green) and then for PI4P (red). (E) Cells were treated as in A and cell-lysate was run on SDS-PAGE and blotted for NS5A and Actin. ****$p<0.0001$; ns, not significant.

in PI4P levels with or without DCV treatment. Surprisingly, hyperphosphorylation of NS5A was not affected in either the WT or Y93H mutant upon DCV treatment (Fig. 9C and D). As was previously shown, the HIT-AAA mutant had increased NS5A hyperphosphorylation (Reiss et al., 2013). Interestingly, DCV treatment decreased the accumulation of NS5A hyper-phosphorylation in the NS5A HIT-AAA mutant (Fig. 9C and D).

Discussion

Previously, we and others have shown that NS5 A interacts with and stimulates PI4KA for efficient replication (Reiss et al., 2011; Berger et al., 2011; Tai and Salloum, 2011; Bianco et al., 2012). Impairment of PI4KA function in HCV replication, either by siRNAs or pharmacological inhibitors, perturbs HCV replication

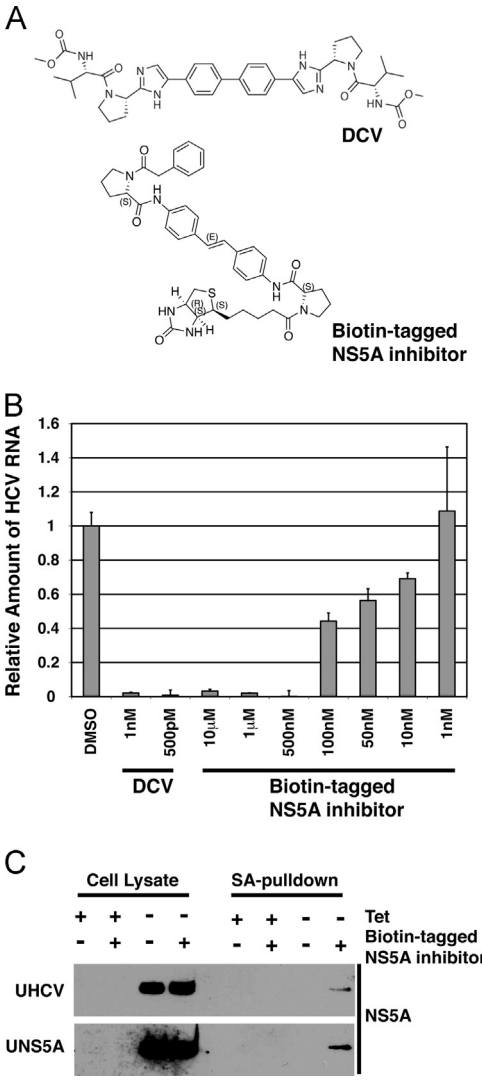

Fig. 6. Biotin-tagged NS5A inhibitor pulls down NS5A from both UHCV and UNS5A with similar efficiencies. (A) Structure comparison of DCV and biotin-tagged NS5A inhibitor. (B) Huh 7.5 cells were electroporated with HCV RNA and treated with either DMSO, DCV or biotin-tagged NS5A inhibitor and RNA is extracted 72 h post-electroporation and HCV RNA was quantified using real time PCR using the $2^{-\Delta\Delta Ct}$ method. (C) UHCV cells and UNS5A cells were induced or left uninduced for 72 h and were either treated with DMSO or biotin-tagged NS5A inhibitor. Cells were lysed and biotin-tagged inhibitor was precipitated using streptavidin dynabeads. Amount of NS5A that was pulled down with the drug was detected by western blotting.

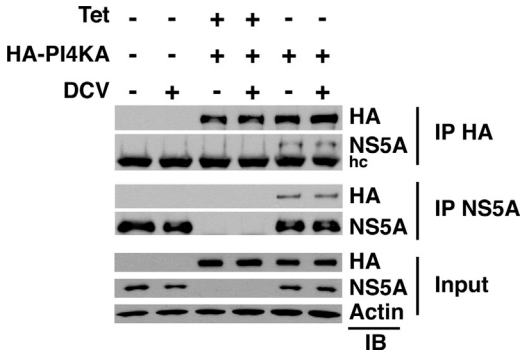

Fig. 7. DCV does not inhibit NS5A–PI4KA interaction. UHCV cells were transduced with retroviral particles containing HA–PI4KA. 24 h later, cells were induced or uninduced for HCV polyprotein expression for 48 h, then treated with DMSO or DCV (1 μM) for 24 h before lysing cells and immunoprecipitating using HA or NS5A antibodies. The immunoprecipitated samples were blotted for HA or NS5A. The bottom panel (input) represents crude cell lysates prior to immunoprecipitation. hc=heavy chain of the antibody.

compartment formation. PI4KA inhibition aggregates the HCV replicase, resulting in large clusters of double membrane vesicles with reduced individual diameter. PI4KA appears to have multiple functions in HCV replication. Its direct product, PI4P, functions in recruiting cellular lipid transfer proteins to the HCV replication compartment. In particular, the cholesterol transporter oxysterol-binding protein (OSBP) binds PI4P, localizes to the HCV replication compartment, and is required for optimal HCV replication (Wang et al., 2014). Additionally, PI4KA modulates the phosphorylation status of NS5 A, either directly or indirectly. In the absence of PI4KA, there is an increased accumulation of hyperphosphorylated NS5 A (Reiss et al., 2013).

In this study, we investigated the effect of DCV on NS5 A motility and the NS5A–PI4KA interaction. Using both a genotype 1a polyprotein inducible system (UHCV) and genotype 2a infection, we show evidence that PI4P accumulation is drastically reduced in DCV-treated cells (Figs. 3 and 7). In addition, we show that in both systems, viral replicase components aggregate during DCV treatment similar to what was previously described in PI4KA knockdown cells (Figs. 1, 2 and 7) (Reiss et al., 2011; Berger et al., 2011). The accumulation of NS5A into large fluorescent foci following DCV treatment is kinetically associated with decreases in NS5A velocities (Fig. 2).

NS5A DAAs have been shown to affect some, but not all, activities associated with NS5A. DCV impairs replication compartment formation and virion assembly, but other functions, such as RNA binding and dimerization, are largely unaffected (Lee et al., 2011; Targett-Adams et al., 2011; Lim et al., 2012). Though it has been recently suggested that NS5A inhibitors compete out oligos for NS5A binding (Ascher et al., 2014), no such competition was seen for HCV 3′ UTR RNA sequence (Targett-Adams et al., 2011). In this study, we define distinct NS5A–PI4KA interactions that are both resistant and sensitive to DCV treatment. The initial interactions of NS5A with PI4KA, including a physical interaction as defined by co-immunoprecipitation, and a modest stimulation of PI4P accumulation away from the Golgi in cells expressing NS5A alone are largely resistant to DCV inhibition. In contrast, later functions associated with the NS5A–PI4KA interaction, including hyper-accumulation of PI4P and appropriate replication compartment formation are inhibited by DCV. Interestingly, the latter DCV-inhibited NS5A functions require NS5A expression to be in the context of the HCV polyprotein. This suggests either that additional HCV proteins are directly involved in the modulation of PI4KA by NS5A or alternatively, that NS5A achieves a certain protein conformation only in the context of other HCV proteins.

An alternative interpretation is that DCV might inhibit other NS5A functions associated with maintaining PI4P pools, such as binding ArfGAP1, which was reported to influence PI4P levels by removing the lipid phosphatase Sac1 from replication compartments (Li et al., 2014). The ArfGAP1 inhibitor, QS11, inhibits HCV replication and reduces the level of PI4P in NS5A expressing cells. This experiment is somewhat difficult to interpret, however, as NS5A alone is less efficient in stimulating PI4P production compared to full-length HCV polyprotein. We examined QS11 and confirmed that it inhibits HCV replication (Fig. S2C). However, it had no effect on PI4P accumulation in UHCV cells that express full-length HCV polyprotein (Fig. S2A and B). Thus, the inhibition of PI4P hyper-accumulation by DCV likely results from inhibiting NS5A conformational changes associated with PI4KA stimulation and not via an effect on ArfGAP1.

Structural and biophysical studies suggest that DCV binds to a dimeric state of NS5A and influences overall structure of NS5A and

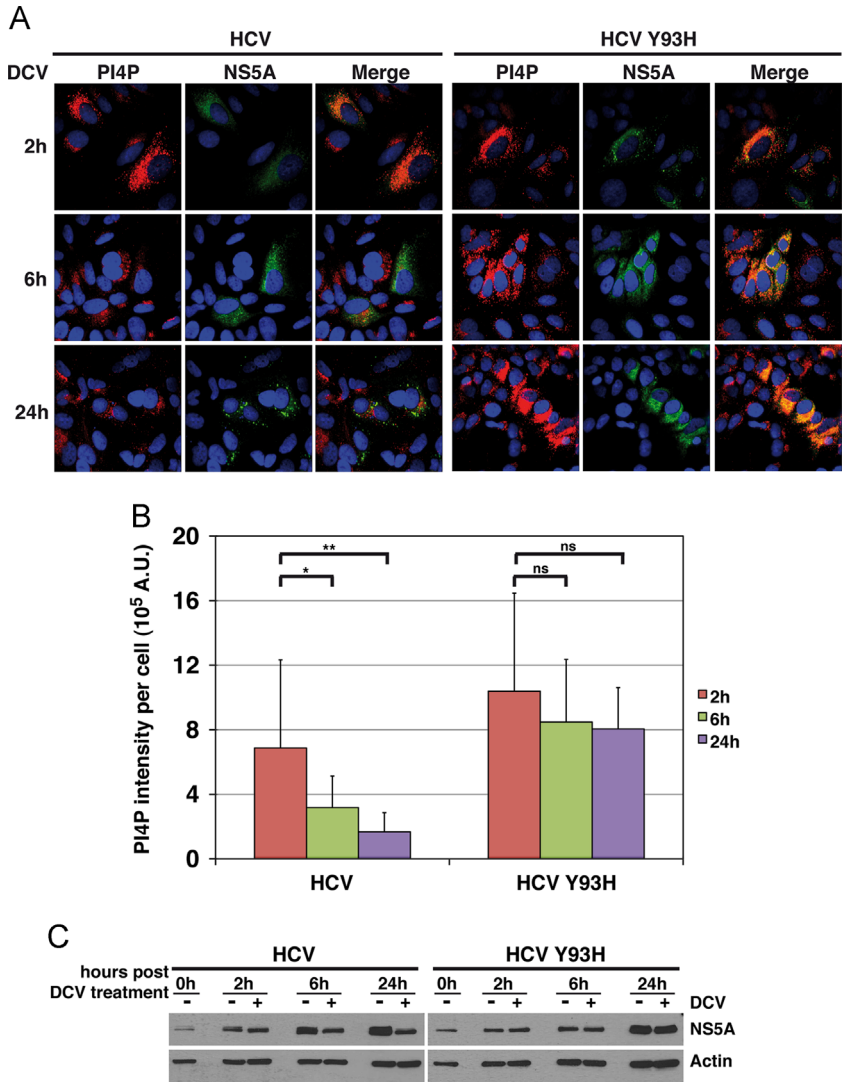

Fig. 8. DCV-resistant mutant Y93H rescues PI4P production in DCV-treated cells. Huh 7.5 cells were infected with either WT or Y93H J6/JFH1 (2a) virus for 48 h and then treated with either DMSO (not shown) or DCV (500pM) for 2, 6 and 24 h prior to fixing and staining for PI4P and NS5A as in Fig. 3. (A) Representative images of each condition are shown. (B) Quantification of PI4P intensity per cell. Error bars represent standard deviation between cells. ns, not significant; $*p < 0.05$; $**p < 0.01$. (C) Cells were treated as in (A) and cell lysate was analyzed by SDS-PAGE and blotted for NS5A and Actin.

that the resistant mutants that arise reduce the affinity of the drug to NS5A (Ascher et al., 2014; Lambert et al., 2014; Bhattacharya et al., 2014; Barakat et al., 2014; O'Boyle et al., 2013). Thus by altering the structural integrity or flexibility of NS5A, DCV might affect not just one but multiple functions of NS5A. In addition to inhibition of HCV assembly, genetic trans-complementation assays using a drug-resistant NS5A suggest that DCV inhibits both cis and trans functions of NS5A in replication (Fridell et al., 2011). Thus, there are at least two NS5A functions in HCV RNA replication that are inhibited by DCV. Domain I of NS5A exists in two different conformations based on structural analysis (Love et al., 2009; Tellinghuisen et al., 2005). Recently, Ascher et al. showed that the DCV binds and locks NS5A Domain 1 in one of the conformations (Ascher et al., 2014). Based on our data, this would suggest that the NS5A conformation that DCV binds is also the conformation that binds PI4KA. The second NS5A conformation, which DCV prevents, would then be associated with PI4KA hyper-stimulation and appropriate replication compartment formation. It is not clear that PI4KA hyper-stimulation and HCV replication compartment formation are functionally linked, since they can be uncoupled under certain conditions (Reiss et al., 2013). In addition, PI4KA has multiple interaction sites for NS5A (Harak et al., 2014). Thus, it is likely that in the presence of DCV, PI4KA can still interact with NS5A with one of the several interaction motifs but is unable to be activated efficiently due to the structural constraint caused by DCV.

Interestingly, a cyclophilin A (CypA) inhibitor was recently found to also perturb HCV replication compartment formation (Madan et al., 2014). CypA binds NS5A and promotes NS5A cis–trans isomerization, which is thought to promote conformational changes. Given the similarities between CypA inhibitors and NS5A DAAs in terms of their effect on HCV replication compartment formation and potential effects on NS5A conformational changes, we propose that both likely share similarities in terms of the mechanism of action for inhibition of HCV replication compartment formation. NS5A DAAs may prevent CypA-dependent conformational changes in NS5A that promote replication compartment formation and PI4KA hyper-stimulation. This common mechanism of HCV inhibition by CypA inhibitors and NS5A DAAs highlights the fact that cellular and viral factors involved in HCV replication compartment formation are a rich source for antiviral drug development (Chukkapalli and Randall, 2014).

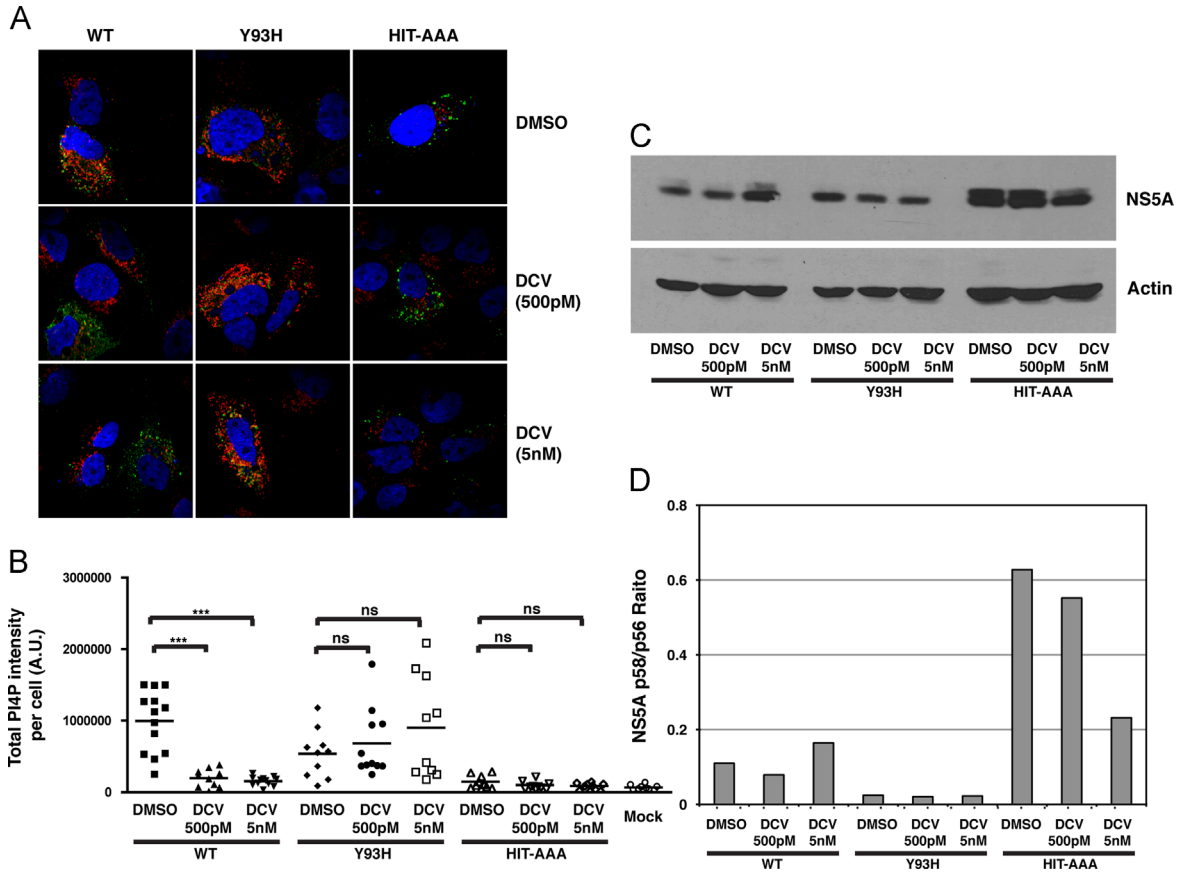

Fig. 9. PI4P and NS5A phosphorylation differences upon DCV treatment in T7RP cells. T7RP cells were transfected with NS3-5B expression plasmids containing WT, Y93H or HIT-AAA NS5A. Four hours post-transfection, cells were treated with DMSO or DCV (500 pM or 5 nM) and 24 h post-transfection cells were fixed (A) or lysed (C). (A) Cells were treated as above and detected using indirect immunofluorescence via sequential staining first for NS5A (green) and then for PI4P (red). (B) PI4P intensity per cell is quantified using Image J. (C) Cells were treated as above and run on an SDS-PAGE to detect phosphorylation differences in NS5A. (D) Ratio of p58/p56 NS5A bands quantified using Image J.

Conclusions

In this study, we show evidence that PI4P hyper-accumulation seen in HCV polyprotein expressing cells is drastically reduced in DCV-treated cells. However, DCV is unable to impair early events of the NS5A–PI4KA interaction that can occur when NS5A is expressed alone. In addition, DCV inhibits replicase formation. Altogether, the data are most consistent with a model wherein DCV inhibits conformational changes in the NS5A protein or protein complex formations that occur in the context of HCV polyprotein expression. These NS5A conformational changes are likely required to both stimulate PI4P hyper-accumulation and form HCV replication compartment.

Materials and methods

Cells

U2OS osteosarcoma derived cell line with tetracycline inducible expression of either full-length genotype 1a polyprotein (UHCV) or NS5A alone (UNS5A) (kindly provided by Darius Moradpour) was cultured in DMEM-high Glucose (Invitrogen Cat. No.: 11995) with 10% fetal bovine serum (FBS), 1 μg/ml Puromycin, 500 μg/ml Geneticin and 1% Penicillin–Streptomycin (PS) along with 1 μg/ml Tetracycline to repress HCV protein expression (Berger et al., 2011; Moradpour et al., 1998). To induce HCV protein expression, cells were washed 3–4 times before adding the above media without tetracycline. Huh-7.5 and HEK 293 T cells were maintained as previously described in DMEM containing 5% FBS, 0.1 mM non-essential amino acids and 1% PS (Berger et al., 2011). T7 RNA polymerase expressing Huh-7.5.1. cells (T7RP cells) (kindly provided by Andrew Tai) are maintained in DMEM with 10% FBS, 0.1 mM non-essential amino acids, 1% PS along with 1.5 μg/ml Puromycin (Tai and Salloum, 2011).

Plasmids and viruses

pTRIP–HA–PI4KA was made by standard restriction enzyme digestion and ligation by replacing PI4KA from pTRIP–PI4KA (previously described (Berger et al., 2011)) with HA-tagged PI4KA from pEF–HA–PI4KA. pJFHxJ6CNS2C3 (NS2/3) was previously described and is similar to JC1 virus (Mateu et al., 2008; Pietschmann et al., 2006). pNS2/3 Y93H carrying DCV-resistant mutation in NS5A was made by PCR mutagenesis and In-fusion HD (Clontech) based cloning. Briefly NS2/3 was digested using SpeI and RsrII and the vector fragment (~9000 bp) was gel purified and used for cloning the two PCR product inserts using In-fusion HD. Two PCR fragments were amplified from wildtype NS2/3 using Phusion high-fidelity DNA polymerase (NEB) using Forward Primer I: CCAGGGGTACAAAGTACTAGTGC, Reverse Primer I: CTGGCCCTCCGTGTgGCAATTGATAGGAAAG; Forward Primer II: CTTTCCTATCAATTGCcACACGGAGGGCCAG, Reverse Primer II: GCTCACCAGGGGACGTCGGAC. The mutation inserted during PCR that changes the genetic code for tyrosine to histidine is shown in lower case. The final plasmid was sequenced to ensure that no additional mutations were inserted during PCR. Infectious genotype 2a virus stock of WT or Y93H mutant was made by electroporating Huh-7.5 cells with either RNA transcribed from NS2/3 or NS2/3 Y93H respectively as described

previously(Mateu et al., 2008; Randall et al., 2006). NS2/3 NS5AeYFP was made by inserting an enhanced yellow fluorescent protein (eYFP) at the previously described site in domain III (SSMPP\widehatLEGEPG) that allows replication of the virus (Moradpour et al., 2004). To facilitate efficient replication, as previously described, residues 2242–2266 in NS5A domain II were deleted (Gottwein et al., 2011). Real-time RT-PCR analysis to determine the amount of HCV RNA was performed as previously described (Berger et al., 2011) and the RNA was quantified using $2^{-\Delta\Delta CT}$ relative quantification method. pTM1 vector (kindly provided by Bernard Moss) was used to clone in NS3-5B from pNS2/3 (genotype 2a) to express the non-structural proteins in T7RP cells. DCV resistant NS5A mutant Y93H and PI4KA-interaction NS5A mutant, HIT-AAA (208–210 amino acids) were made by standard PCR-based cloning.

Chemicals and antibodies

Daclatasvir (DCV) (Selleck Chemicals) was dissolved in DMSO and diluted in media to the final concentration used for the assays. Wortmannin (Sigma) was dissolved in DMSO and used at the concentrations described in figure legends. Digitonin (Sigma) was dissolved in PBS and made fresh before each use.

Primary antibodies used include: rabbit anti-GM130 (Abcam Cat. No.: ab52649), mouse anti-PI4P (Echelon biosciences Cat. No: ZP004), mouse anti-NS5A (9E10: a kind gift from Charles Rice, Rockefeller University), mouse anti-NS5B (Enzo life sciences Cat. No.: ALX-803-061), rabbit anti-Actin (Sigma Cat. No.: A2066), and mouse anti-HA (Covance Cat. No.: MMS-101R). Alexafluor-488 conjugated Wheat germ agglutinin (WGA) (Invitrogen) was diluted to a 1 mg/ml stock solution in PBS.

Immunofluorescence

Glass coverslips in 24-well plates were coated with 100 μg/ml poly-L-lysine for 10 min, washed with sterile water and dried. 30,000 UHCV cells and 20,000 UNS5A cells were seeded and induced for 72 h or for 96 h respectively before fixing. For intracellular PI4P staining, cells were fixed in 4% paraformaldehyde, permeabilized with 20 μM digitonin for 5 min, and quenched with 50 mM ammonium chloride for 15 min. Cells were then blocked with 20% normal goat serum (NGS) for 30 min. All primary and secondary antibodies were diluted in 10% NGS. When using mouse anti-PI4P IgM in combination with mouse anti-NS5A IgG, cells were stained first with NS5A (1:20,000) and detected by anti-mouse IgG Alexa Fluor 488 (1:1000) and were then further blocked and stained for PI4P (1:200) and detected by anti-mouse IgM Alexa Fluor 594 (1:1000). When staining for NS5B in combination with NS5A, cells were fixed with 4% PFA and permeabilized with 0.1% Triton-X-100 and blocked with 20% NGS. Cells were first stained for NS5B (1:200) and detected using anti-mouse IgG Alexa Fluor 594 and then stained for NS5A using Alexa Fluor-488 conjugated 9E10 (1:100) (Invitrogen APEX antibody labeling kit). For plasma membrane staining of PI4P, cells were first incubated with 50 μg/ml Alexa Fluor-488 conjugated Wheat Germ Agglutinin on ice for 5 min before fixing with 4% formaldehyde and 0.2% glutaraldehyde and rinsing with 50 mM ammonium chloride (NH_4Cl). Permeabilization, blocking and staining were carefully performed on ice with pre-chilled reagents as described by Hammond et al. (2009). Briefly, cells were blocked and permeabilized with Buffer A (20 mM PIPES, pH 6.8, 137 mM NaCl, 2.7 mM KCl) containing 5% NGS, 50 mM NH_4Cl and 0.5% saponin for 45 min on ice. After a couple of rinses with buffer A on ice, primary antibodies were applied in buffer A with 5% NGS and 0.1% saponin for 1 h on ice. After two washes, secondary antibody was applied in the same buffer as primary and incubated for 45 min on ice. The cells were then washed four times in buffer A and post-fixed in 2% formaldehyde in PBS for 10 min on ice and warmed to RT for additional 5 min and rinsed three times in PBS containing 50 mM NH_4Cl and once in distilled water before mounting. After staining, all coverslips were mounted in ProLong Gold anti-fade with Dapi nuclear stain (Invitrogen). Samples were imaged using Olympus DSU spinning disc confocal microscope equipped with Photometrics Evolve EMCCD camera. (UChicago Microscopy core facility). Images were taken and processed using SlideBook v5.0 software and analyzed using Image J (NIH).

Immunoprecipitation and western blotting

Immunoprecipitation of PI4KA and NS5A was performed as previously described (Berger et al., 2011). Briefly, HEK 293T cells were transfected with pTRIP–HA–PI4KA, HIV–Gagpol and VSV glycoprotein using Lipofectamine 2000. Supernatant containing pTRIP–HA–PI4KA pseudoparticles was collected 48 h later and used to transduce UHCV cells. Twenty-four hours post-transduction, cells were induced for HCV polyprotein expression or left uninduced for a total of 48 h. Cells were treated with 250 pM DCV or DMSO 24 h post-induction for a total of 24 h. Cells were lysed on ice for 30 min in NP-40 lysis buffer (20 mM Tris–HCl, pH7.5, 150 mM NaCl, 2 mM EDTA, 1% Nonidet P-40, 10% Glycerol supplemented with complete protease inhibitor cocktail tablets from Roche), clarified by centrifugation at 20,000*g* for 30 min. The supernatant was mixed with M-280 sheep anti-mouse IgG dynabeads (Invitrogen) conjugated with either NS5A 9E10 antibody or HA antibody to immunoprecipitate NS5A and HA–PI4KA respectively. During overnight immunoprecipitation at 4 °C, DCV-treated cells were further treated with 0.6 nM DCV. The immune-complexes were washed three times in NP40-lysis buffer and boiled with 1 × Laemelli buffer for 5 min before loading on the gel, along with 1% of input cell lysate and blotted for NS5A, HA–PI4KA and Actin.

Synthesis of biotinylated NS5A inhibitor

(*E*)-Di-tert-butyl-2,2′-(((ethene-1,2-diylbis(4,1-phenylene))bis (azanediyl))bis(carbonyl))bis(pyrrolidine-1-carboxylate) (1). To a solution of 4,4′-diaminostilbene dihydrochloride (60 mg, 0.21 mmol) in DCM (1 ml) potassium carbonate (58 mg, 0.42 mmol) was added, and the resulting mixture was stirred at RT for 30 min. Ethyl-2-ethoxyquinoline-1-(2H)-carboxylate (125 mg, 0.50 mmol) and N-Boc proline (104 mg, 0.48 mmol) were added and the mixture was stirred at RT for 6 h. The solvent was removed under vacuum and the residue was triturated in ethyl ether. The products were isolated by filtration, washed with H_2O and ethyl ether, and dried under vacuum. The coupling product **1** was obtained as a white solid in 95% yield (120 mg, 0.19 mmol). ^{1}H NMR (300 MHz, DMSO-d6): δ=10.08 (s, 2H), 7.61–7.48 (m, 4H), 7.07 (s, 2H), 4.21–4.09 (m, 2H), 3.34–3.28 (m, 4H), 2.33–2.12 (m, 2H), 1.98–1.70 (m, 6H), 1.38 (s, 9H), 1.25 (s, 9H), HRMS-ESI (m/z) calcd for $C_{34}H_{45}N_4O_6$ [M-H]+: 605.7443, found: 605.3358. (*E*)-N,N′-(ethene-1,2-diylbis (4,1-phenylene))bis(pyrrolidine-2-carboxamide) (2). TFA (0.15 ml) was added slowly to a solution of **1** (60 mg, 0.01 mmol) in DCM (1.4 ml). The reaction mixture was stirred at RT for 4 h. The solvent was removed under vacuum, the residue was dissolved in ethyl acetate (4 ml), washed with 1 M NaOH (2 ml) and brine (2 ml), dried over Na_2SO_4, filtered, and concentrated to afford **2** as a yellow solid in 99% yield (39 mg, 0.09 mmol) which was further used without purification. ^{1}H NMR (300 MHz, DMSO-d6): δ=9.97 (s, 2H), 7.62 (d, J=8.7 Hz, 2H), 7.48 (d, *J*=8.4 Hz, 2H), 7.07 (s, 2H), 3.40–3.32 (m, 2H), 2.86 (t, *J*=6.6 Hz, 4H), 2.10–1.99 (m, 2H), 1.98–1.62 (m, 6H), HRMS-ESI (m/z) calcd for $C_{24}H_{29}N_4O_2$ [M-H]+: 404.5127, found: 405.2305. (*E*)-1-(2-phenylacetyl)-N-(4-(4-(pyrrolidine-2-carboxamido)styryl)phenyl)pyrrolidine-2-carboxamide (3). Triethyl amine (0.014 ml, 0.09 mmol) was added to a solution of **2** (30 mg,

0.07 mmol) in DCM (0.6 ml) at 0 °C. To this mixture a solution of phenylacetylchloride (0.07 ml, 0.05 mmol) in DCM (0.1 ml) was added and the reaction was stirred at RT for 4 h. The reaction mixture was diluted with DCM (5 ml), washed with H_2O (3 ml), $NaHCO_3$ (3 ml), and brine (3 ml), dried over Na_2SO_4, filtered, and concentrated. The crude product was purified by silica gel chromatography with 5% MeOH in DCM as the eluent, affording **4** as a white solid in 52% yield (13 mg, 0.02 mmol). ^{1}H NMR (300 MHz, $CDCl_3$): δ=7.59–7.49 (m, 10 H), 7.31–7.28 (m, 3H), 7.06 (d, J=7.2 Hz, 2H), 4.60–4.56 (m, 1H), 4.04–3.99 (m, 1H), 3.78 (s, 2H), 3.76–3.58 (m, 4H), 3.28–3.12 (m, 2H), 2.07–1.89 (m, 6H), HRMS-ESI (m/z) calcd for $C_{32}H_{35}N_4O_3$ [M-H]+: 523.6453, found: 523.2736. (2*S*)-1-5-((3aS,4S,6aR)-2-oxohexahydro-1H-thieno(Stedman, 2014; imidazol-4-yl)pentanoyl)-N-(4-((*E*)- 2-(4-((((2S)-1-(phenylacetyl)-2-pyrrolidinyl)carbonyl)amino)phenyl)vinyl)phenyl)-2-pyrrolidinecarboxamide (4). DIPEA (0.036 ml, 0.21 mmol) and biotin-NHS (14.5 mg, 0.04 mmol) were added to a solution of **3** (22 mg, 0.04 mmol) in DMF (0.3 ml). The reaction mixture was stirred overnight at RT and was slowly poured into vigorously stirred cold ethyl ether (6 ml). The solid was isolated by filtration, washed with cold ethyl ether (4 ml) and dried under vacuum to afford the product **4** as a white solid in 47% yield. ^{1}H NMR (300 MHz, DMSO-d6): δ=10.04 (s, 2H), 7.94 (s, 1H), 7.59–7.48 (m, 6H), 7.29–7.08 (m, 6H), 6.35 (d, J=8.9 Hz, 2H), 4.45–4.06 (m, 4H), 3.69 (s, 2H), 3.66–4.40 (m, 4H), 3.15–2.99 (m, 1H), 2.87–2.76 (m, 2H), 2.64–1.90 (m, 8H), 1.70–1.20 (m, 8H), 1.10–1.07 (m, 2H), HRMS-ESI (m/z) calcd for $C_{42}H_{49}N_6O_5S$ [M-H]+: 749.9407, found: 749.3520. The analytical data is consistent with literature data (Gao et al., 2010). The synthesis scheme is shown in Fig. S1.

Streptavidin pull-down

UHCV cells and UNS5A cells were induced or left uninduced for 72 h. Cells were treated with either DMSO or biotinylated NS5A inhibitor (1 μM) for 16 h before lysis. Cells were lysed in NP-40 lysis buffer and biotinylated NS5 A inhibitor was precipitated using M280-streptavidin dynabeads (Invitrogen) overnight at 4 °C and washed four times in NP-40 lysis buffer and loaded on the gel along with 1% cell lysate.

Statistical analysis

Student's *t*-test was performed to compare data sets. *P*-values less than 0.05 were considered significant.

Acknowledgments

We thank Charles Rice (The Rockefeller University, New York), Takaji Wakita (National Institutes of Infectious Diseases, Tokyo), Darius Moradpour (University of Lausanne, Switzerland), Andrew Tai (University of Michigan), and Bernard Moss (NIH) for providing reagents. We thank The University of Chicago Light Microscopy Facility director Vytas Bindokas and Christine Labno. We thank our laboratory members for their critical input and reading of the manuscript. This work is supported by NIAID (1R01AI080703), the American Cancer Society (118676-RSG-10-059-01-MPC to G.R. and 120130-RSG-11-066-01-RMC to A.D.), Susan and David Sherman to G.R. and by American Heart Association postdoctoral fellowship to V.C.

Appendix A. Supporting information

Supplementary data associated with this article can be found in the online version at http://dx.doi.org/10.1016/j.virol.2014.12.018.

References

Appel, N., et al., 2008. Essential role of domain III of nonstructural protein 5A for hepatitis C virus infectious particle assembly. PLoS. Pathog. 4 (3), e1000035.
Ascher, D.B., et al., 2014. Potent hepatitis C inhibitors bind directly to NS5A and reduce its affinity for RNA. Sci. Rep. 4, 4765.
Au, J.S., Pockros, P.J., 2014. Novel therapeutic approaches for hepatitis C. Clin. Pharmacol. Ther. 95 (1), 78–88.
Balla, A., et al., 2005. A plasma membrane pool of phosphatidylinositol 4-phosphate is generated by phosphatidylinositol 4-kinase type-III alpha: studies with the PH domains of the oxysterol binding protein and FAPP1. Mol. Biol. Cell 16 (3), 1282–1295.
Barakat, K.H., et al., 2014. A refined model of the HCV NS5A protein bound to daclatasvir explains drug-resistant mutations and activity against divergent genotypes. J. Chem. Inf. Model. (Epub ahead of print, April 14, 2014).
Berger, K.L., Randall, G., 2009. Potential roles for cellular cofactors in hepatitis C virus replication complex formation. Commun. Integr. Biol. 2 (6), 471–473.
Berger, K.L., et al., 2009. Roles for endocytic trafficking and phosphatidylinositol 4-kinase III alpha in hepatitis C virus replication. Proc. Natl. Acad. Sci. USA 106 (18), 7577–7582.
Berger, K.L., et al., 2011. Hepatitis C virus stimulates the phosphatidylinositol 4-kinase III alpha-dependent phosphatidylinositol 4-phosphate production that is essential for its replication. J. Virol. 85 (17), 8870–8883.
Bhattacharya, D., et al., 2014. Pharmacological disruption of hepatitis C NS5A protein intra- and intermolecular conformations. J. Gen. Virol. 95 (Pt 2), 363–372.
Bianco, A., et al., 2012. Metabolism of phosphatidylinositol 4-kinase IIIalpha-dependent PI4P Is subverted by HCV and is targeted by a 4-anilino quinazoline with antiviral activity. PLoS Pathog. 8 (3), e1002576.
Blight, K.J., Kolykhalov, A.A., Rice, C.M., 2000. Efficient initiation of HCV RNA replication in cell culture. Science 290 (5498), 1972–1974.
Borawski, J., et al., 2009. Class III phosphatidylinositol 4-kinase alpha and beta are novel host factor regulators of hepatitis C virus replication. J. Virol. 83 (19), 10058–10074.
Chatel-Chaix, L., et al., 2012. Direct-acting and host-targeting HCV inhibitors: current and future directions. Curr. Opin. Virol..
Chukkapalli, V., Randall, G., 2014. Hepatitis C virus replication compartment formation: mechanism and drug target. Gastroenterology 146 (5), 1164–1167.
Evans, M.J., Rice, C.M., Goff, S.P., 2004. Phosphorylation of hepatitis C virus nonstructural protein 5A modulates its protein interactions and viral RNA replication. Proc. Natl. Acad. Sci. USA 101 (35), 13038–13043.
Eyre, N.S., et al., 2014. Dynamic imaging of the hepatitis C virus NS5A protein during a productive infection. J. Virol. 88 (7), 3636–3652.
Fridell, R.A., et al., 2011. Distinct functions of NS5A in hepatitis C virus RNA replication uncovered by studies with the NS5A inhibitor BMS-790052. J. Virol. 85 (14), 7312–7320.
Gao, M., et al., 2010. Chemical genetics strategy identifies an HCV NS5A inhibitor with a potent clinical effect. Nature 465 (7294), 96–100.
Gosert, R., et al., 2003. Identification of the hepatitis C virus RNA replication complex in Huh-7 cells harboring subgenomic replicons. J. Virol. 77 (9), 5487–5492.
Gottwein, J.M., et al., 2011. Development and application of hepatitis C reporter viruses with genotype 1–7 core-nonstructural protein 2 (NS2) expressing fluorescent proteins or luciferase in modified JFH1 NS5A. J. Virol. 85 (17), 8913–8928.
Guedj, J., et al., 2013. Modeling shows that the NS5A inhibitor daclatasvir has two modes of action and yields a shorter estimate of the hepatitis C virus half-life. Proc. Natl. Acad. Sci. USA 110 (10), 3991–3996.
Hammond, G.R., Schiavo, G., Irvine, R.F., 2009. Immunocytochemical techniques reveal multiple, distinct cellular pools of PtdIns4P and PtdIns(4,5)P(2). Biochem. J. 422 (1), 23–35.
Harak, C., et al., 2014. Mapping of functional domains of the lipid kinase phosphatidylinositol 4-kinase type III alpha involved in enzymatic activity and hepatitis c virus replication. J. Virol..
He, Y., K.A. Staschke, S.L. Tan, 2006. HCV NS5A: a multifunctional regulator of cellular pathways and virus replication. In: , Tan,S.L. (Ed). Hepatitis C Viruses: Genomes and Molecular Biology, Norfolk, UK.
Huang, Y., et al., 2007. Phosphorylation of hepatitis C virus NS5A nonstructural protein: a new paradigm for phosphorylation-dependent viral RNA replication. Virology 364 (1), 1–9.
Kaneko, T., et al., 1994. Production of two phosphoproteins from the NS5A region of the hepatitis C viral genome. Biochem. Biophys. Res. Commun. 205 (1), 320–326.
Lambert, S.M., et al., 2014. The crystal structure of NS5A domain 1 from genotype 1a reveals new clues to the mechanism of action for dimeric HCV inhibitors. Protein Sci. 23 (6), 723–734.
Lee, C., et al., 2011. The hepatitis C virus NS5A inhibitor (BMS-790052) alters the subcellular localization of the NS5A non-structural viral protein. Virology 414 (1), 10–18.
Lemm, J.A., et al., 2010. Identification of hepatitis C virus NS5A inhibitors. J. Virol. 84 (1), 482–491.
Li, H., et al., 2014. Hepatitis C virus NS5A Hijacks ARFGAP1 to maintain a phosphatidylinositol 4-phosphate-enriched microenvironment. J. Virol. 88 (11), 5956–5966.
Li, Q., et al., 2009. A genome-wide genetic screen for host factors required for hepatitis C virus propagation. Proc. Natl. Acad. Sci. USA 106 (38), 16410–16415.

Lim, P.J., et al., 2012. Correlation between NS5A dimerization and Hepatitis C virus replication. J. Biol. Chem. 287 (36), 30861–30873.
Lohmann, V., et al., 2003. Viral and cellular determinants of hepatitis C virus RNA replication in cell culture. J. Virol. 77 (5), 3007–3019.
Love, R.A., et al., 2009. Crystal structure of a novel dimeric form of NS5A domain I protein from hepatitis C virus. J. Virol. 83 (9), 4395–4403.
Madan, V., et al., 2014. Inhibition of HCV replication by cyclophilin antagonists is linked to replication fitness and occurs by inhibition of membranous web formation. Gastroenterology 146 (5), 1361–1372 (e1-9).
Mateu, G., et al., 2008. Intragenotypic JFH1 based recombinant hepatitis C virus produces high levels of infectious particles but causes increased cell death. Virology 376 (2), 397–407.
McGivern, D.R., et al., 2014. Kinetic analyses reveal potent and early blockade of Hepatitis C virus assembly by NS5A inhibitors. Gastroenterology.
Moradpour, D., Penin, F., 2013. Hepatitis C virus proteins: from structure to function. Curr. Top. Microbiol. Immunol. 369, 113–142.
Moradpour, D., et al., 1998. Continuous human cell lines inducibly expressing hepatitis C virus structural and nonstructural proteins. Hepatology 28 (1), 192–201.
Moradpour, D., et al., 2004. Insertion of green fluorescent protein into nonstructural protein 5A allows direct visualization of functional hepatitis C virus replication complexes. J. Virol. 78 (14), 7400–7409.
O'Boyle Ii, D.R., et al., 2013. Characterizations of HCV NS5A replication complex inhibitors. Virology 444 (1-2), 343–354.
Penin, F., et al., 2004. Structure and function of the membrane anchor domain of hepatitis C virus nonstructural protein 5A. J. Biol. Chem. 279 (39), 40835–40843.
Pietschmann, T., et al., 2006. Construction and characterization of infectious intragenotypic and intergenotypic hepatitis C virus chimeras. Proc. Natl. Acad. Sci. USA 103 (19), 7408–7413.
Qiu, D., et al., 2011. The effects of NS5A inhibitors on NS5A phosphorylation, polyprotein processing and localization. J. Gen. Virol. 92 (Pt 11), 2502–2511.
Randall, G., et al., 2006. Silencing of USP18 potentiates the antiviral activity of interferon against hepatitis C virus infection. Gastroenterology 131 (5), 1584–1591.
Reiss, S., et al., 2011. Recruitment and activation of a lipid kinase by hepatitis C virus NS5A is essential for integrity of the membranous replication compartment. Cell Host Microbe 9 (1), 32–45.
Reiss, S., et al., 2013. The lipid kinase phosphatidylinositol-4 kinase III alpha regulates the phosphorylation status of hepatitis C virus NS5A. PLoS Pathog. 9 (5), e1003359.
Stedman, C., 2014. Sofosbuvir, a NS5B polymerase inhibitor in the treatment of hepatitis C: a review of its clinical potential. Ther. Adv. Gastroenterol. 7 (3), 131–140.
Tai, A.W., Salloum, S., 2011. The role of the phosphatidylinositol 4-kinase PI4KA in hepatitis C virus-induced host membrane rearrangement. PLoS One 6 (10), e26300.
Tai, A.W., et al., 2009. A functional genomic screen identifies cellular cofactors of hepatitis C virus replication. Cell Host Microbe 5 (3), 298–307.
Targett-Adams, P., et al., 2011. Small molecules targeting hepatitis C virus-encoded NS5A cause subcellular redistribution of their target: insights into compound modes of action. J. Virol. 85 (13), 6353–6368.
Tellinghuisen, T.L., Marcotrigiano, J., Rice, C.M., 2005. Structure of the zinc-binding domain of an essential component of the hepatitis C virus replicase. Nature 435 (7040), 374–379.
Trotard, M., et al., 2009. Kinases required in hepatitis C virus entry and replication highlighted by small interference RNA screening. FASEB J. 23 (11), 3780–3789.
Vaillancourt, F.H., et al., 2009. Identification of a lipid kinase as a host factor involved in hepatitis C virus RNA replication. Virology 387 (1), 5–10.
WHO. Available from: ⟨http://www.who.int/mediacentre/factsheets/fs164/en/⟩.
Wang, H., et al., 2014. Oxysterol-binding protein is a phosphatidylinositol 4-kinase effector required for HCV replication membrane integrity and cholesterol trafficking. Gastroenterology 146 (5), 1373–1385 (e1-11).
Wolk, B., et al., 2008. A dynamic view of hepatitis C virus replication complexes. J. Virol. 82 (21), 10519–10531.